

# Slip weakening, strain and short-term preseismic disturbances

Vitali A. Morgounov

*The Head of Tectono-Electromagnetic Laboratory, Schmidt United Institute of Physics of the Earth,  
Russian Academy of Sciences, Moscow, Russia*

## Abstract

The problem of short-term earthquake precursors is discussed. In contrast to the increasing number of reports on short-lived precursors of various types, direct strain measurements cannot detect clearly expressed preseismic anomalies, as follows from the aseismic nucleation mechanism. Based on previously published data and the assumption that the attenuation of the stress-strain field is proportional to  $r^{-3}$ , a possible scenario of the final stage of earthquake nucleation process is proposed on the basis of the slip weakening mechanism in the source and the associated mosaic pattern of precursors on the Earth's surface. The formulas for estimating the maximum distance of precursor detection and minimum duration of the final stage of inelastic deformation preceding brittle failure of rocks are derived. The data of electromagnetic precursors are interpreted in terms of a skin-layer model. A considerable increase in strain rates at the final stage of the earthquake nucleation provides an opportunity to explain teleseismic effects before strong earthquakes in terms of normalized epicenter distance. The modeling results are compared with *in situ* observations.

**Key words** *slip weakening – accelerated creep – short-term earthquake precursor – strain – spatial-temporal scale – mosaic pattern – teleseismic effects*

## 1. Introduction

Several fundamental problems are still unsolved in the problem of earthquake (EQ) prediction. Nevertheless, the optimistic point of view is supported by few successfully predicted destructive EQs (Raleygh *et al.*, 1977; Hui *et al.*, 1997; Sykes *et al.*, 1999). On the other hand, the phenomena of Self-Organized Criticality (SOC) in the Earth's crust (Bak *et al.*, 1988) have no scale length, and hence any reli-

able evaluation of the place, time, and intensity of an EQ is considered to be unlikely. The SOC concept actually denies any progress and brings the problem of EQ prediction back to its initial state (Geller, 1997). Further research is required to clarify whether the SOC is an insurmountable obstacle or it only indicates the inadequacy of available data.

Among various prediction problems, the feasibility of short-term prediction is the least studied and depends on the nature and scale of the aseismic nucleation phase of large EQs (Sykes *et al.*, 1999). The stage of tertiary creep (or slip weakening), which precedes the brittle fracture of rocks, can be regarded as a mechanism of short-term precursor generation. Accelerating strain considerably increases the signal-to-noise ratio of measurable geophysical parameters, which is beneficial to the identification of the ductile failure stage in the source by measuring geophysical fields at the Earth's surface. The creep process develops in an avalanche-like manner and acquires an important

---

*Mailing address:* Prof. Vitali A. Morgounov, The Head of Tectono-Electromagnetic Laboratory, Schmidt United Institute of Physics of the Earth, Russian Academy of Sciences, ul. Bolshaya Gruzinskaya 10, D-242, GSP-5, 123995 Moscow, Russia; e-mail: vam@ifz.ru

property of irreversibility. This scenario of EQ development appears to be logically consistent.

However, in spite of the encouraging experimental results of short-term precursor studies (Fleischer, 1981; Warwick *et al.*, 1982; Oki *et al.*, 1988; Rikitake, 1988; Roeloffs, 1988; Fraser-Smith *et al.*, 1990; Varotsos *et al.*, 1993; Wakita *et al.*, 1998; Uyeda *et al.*, 2000; Meloni *et al.*, 2001a,b; Tramutoli *et al.*, 2001; Spichak *et al.*, 2002) and theoretical models of faulting according to which the rupture should be preceded by a gradually accelerating slip (Press, 1965; Rice *et al.*, 1979; Dieterich, 1992; Ohnaka, 1993), the strain anomalies have not been reliably established by direct strain measurements before earthquakes in various regions of the Earth and in California in particular (Johnston *et al.*, 1994; Wyatt *et al.*, 1994; Abercrombie, 1995).

The San Andreas sliding fault zone seems to be the most spectacular example of the contradiction. Since the problem in question is of crucial importance, a brief review of *in situ* measurements in this region and the discussion of the related important features (the mosaic pattern of the strain field and teleseismic effects) are presented below.

Along with controversial arguments, many authors report on preseismic irregular patterns observed in the San Andreas zone (O'Neil *et al.*, 1981; Teng *et al.*, 1981; Roeloffs, 1988; Ben-Zion, 1990; Fraser-Smith, 1990). Leary and Malin (1984) observed ground deformation events a few hours before the Homestead Valley sequence of EQs of 1979 in Southern California ( $4.7 < M_L < 5.2$ ); the observations were made at three separate points on the periphery of the Mojave block. These events manifested themselves as anomalous water level variations and a creep step measured by a US Geological Survey creepmeter.

Dodge *et al.* (1996) found that foreshocks of the Landers EQ provide clear evidence for an extended aseismic nucleation process before some EQs. Harris (1998) came to the conclusion that aseismic creep controls the rupture process and the creep process is the key idea of EQ instability models. Wesson and Nicholson (1988) emphasized the importance of the creep loading mechanism and suggested, in particu-

lar, that the Landers foreshock sequence may have been driven by aseismic creep. Johnston and Linde (2002) reviewed the surface observations of episodic displacements on active faults and explained unsuccessful attempts to detect any indications of exponentially increasing strain (tertiary creep or slip weakening) by the fact that the scale of the initial failure must be small compared to the eventual rupture zone.

Evidently, the interpretation of the experimental data is complicated due to such factors as the specific role of the surface layer or the mosaic pattern of the stress field. A significant example is the fact that no precursors were recorded by the strainmeters of the Pinyon Flat Observatory (PFO) at a distance of only 70 km from the epicenter of the Landers EQ ( $M = 7.3$ ) (Wyatt *et al.*, 1994; Abercrombie *et al.*, 1995). The PFO and epicenter were located on the opposite sides of the San Andreas Fault. According to Mount *et al.* (1992), the San Andreas Fault Zone can be considered a weak fault, which in extreme case can be thought of as a free surface and acts as a stress refractor. Wesson *et al.* (1988) consider the California crust not as an elastic half-space but as a mosaic of relatively rigid elastic plates or blocks separated by relatively weak fault zones (this interpretation is similar to the model proposed by Bilham and Beavan, 1979).

### 1.1. Mosaic pattern of the stress field

Water level anomalies during the Landers EQ can serve as a convincing example of a mosaic structure of the strain field. In three of four boreholes in the PFO area, the water level dropped by 0.15 to 0.3 m at the time of the Landers event. In the fourth well, located at a distance of 100-250 m from the other three, the water level dropped over 5 m (Wyatt *et al.*, 1994); *i.e.* observations made at points a few hundred meters apart differ by more than 10 times! It is noteworthy in this context that, according to Mogi (1981), many precursors tend to appear at singular points of tectonic structures. These facts, as well as many other data, confirm the mosaic pattern of the strain field distribution associated with seismic events. It is

evident that a uniform model of the crust is generally inadequate.

Comparing various seismic regions, Mogi (1981) characterized Central California as a homogeneous straight fault zone without any appreciable precursors, in contrast to Japan as a region of complex structures of small dimensions producing noticeable precursors in relatively small areas and some parts of China as a region of complex continental structures of large dimensions where remarkable precursors can be observed in large areas. This is consistent with laboratory experiments showing that the more inhomogeneous the specimen, the earlier the stage at which fracture precursors arise and agrees with the conclusion of Dodge *et al.*, (1996) that the fault zone heterogeneity is an important factor controlling the number of foreshocks (*i.e.* the stronger the heterogeneity, the greater the number of foreshocks).

A complicated mosaic pattern of the strain field was revealed before the North Palm Springs ( $M = 5.6$ ) EQ of 1986 in California. No anomalies were recorded at the Pinon Flat strain Observatory ( $\sim 33$  km from the epicenter) and by the PUBS dilatometer ( $\sim 95$  km from the epicenter), whereas the XWR creepmeter ( $\sim 103$  km from the epicenter and  $\sim 10$  km from the PUBS dilatometer) showed a sharp change in the slope of the creep records that leads the water level excursion recorded by the Phelan water level monitor ( $\sim 65$  km from epicenter). Ben-Zion *et al.* (1990) considered these records as a possible preseismic signal. However, during the Landers EQ of June 28, 1992 (the largest in California during the last 40 years;  $M_w 7.3$ ), the borehole dilatational strainmeter PUBS (a sensitivity of less than a nanostrain) installed at the site about 100 km from 85 km-long Landers rupture and 135 km from the epicenter exhibited no indications of precursive strain at this location due to either precursive slip on the Landers rupture or local slip on the San Andreas (Johnston *et al.*, 1994).

### 1.2. Short-term precursors at teleseismic distances

The mosaic pattern of the strain field creates a specific obstacle to the detection of precursor-

ry events and determination of the spatial scale of the preparation zone. Obviously, the size of the zone largely depends on the EQ magnitude. The first results on anomalous pre-seismic tilts at greater distances (Tomaschek, 1955) cannot be regarded as adequate because of imperfections of the instruments used at that time. However, these data cannot be ignored because similar reports on precursors of various types recorded at great distances were published later. Wideman and Major (1967) recorded strain steps in Colorado at great epicentral distances. Lomnitz *et al.* (1978) reported a radon anomaly preceding Tangshan event ( $M = 7.8$ ) and recorded at a distance of 1800 km. Fleischer (1981) reviewed the geochemical responses to distant EQs and proposed a dislocation model. Preseismic anomalies were recorded by resistivity variometers at distances of more than 1000 km (Rikitake 1976; Yamazaki, 1983; Rikitake and Yamazaki, 1985). Five observatories in the United States recorded an EM emission event a few days before the Great Chilean ( $M = 8.5$ ) EQ of 1960 at epicentral distances of about 10 000 km (Warwick *et al.*, 1982). Based on satellite measurements Tramutoli *et al.* (2001) identified thermal infrared (TIR) anomalous effects at a distance of 400 km from the epicenter of the  $M = 6.9$  November 23, 1980 EQ in Italy.

Teleseismic effects are recognizable from records of strong EQs. However, it is more appropriate to analyze these effects in relative ( $r/R^*$ ), rather than absolute distances (normalized to the radius of preparation zone  $R^*$ ), *i.e.* to compare geometrically similar EQs of different magnitudes. Then, high- and low-energy seismic events can be analyzed in the same terms. This paper is an attempt to consider some consequences of a scenario modeling the final stage of EQ nucleation based on the slip weakening mechanism.

## 2. Spatial scale of short-term seismic precursors

The problems of the ultimate distance of short-lived precursor detection have been extensively studied and several empirical and theoretical formulas have been proposed for the esti-

mation of the size (radius  $R^*$ ) of the preparation zone. Figure 1 illustrates the results of studying the relation  $R^*(M)$  of various geophysical parameters (resistivity, geochemical and electromagnetic characteristics, water level, magnetic field, strain, tidal variations, etc.) within a wide range of the EQ energy ( $4 < M < 8$ ).

Wideman and Major (1967) made an attempt to find the response of the Earth's crust to the nucleation process at teleseismic distances; they derived the relation for the magnitude dependence  $R^*(M)$ , (fig. 1) of strain steps

measured in Colorado during distant EQs ( $3.5 < M < 8.5$ ).

The results by Wideman and Major were criticized from various points of view and were generally considered erroneous in spite of the corroboration their results by other authors (Berger, 1973; Yamada, 1973). Note however that, among tens of cases listed in the catalog of strain steps collected by Yamada (1973), at least five were recorded few hours before EQs, and Rikitake (1976) concluded that these events «were clearly distinct as precursors».

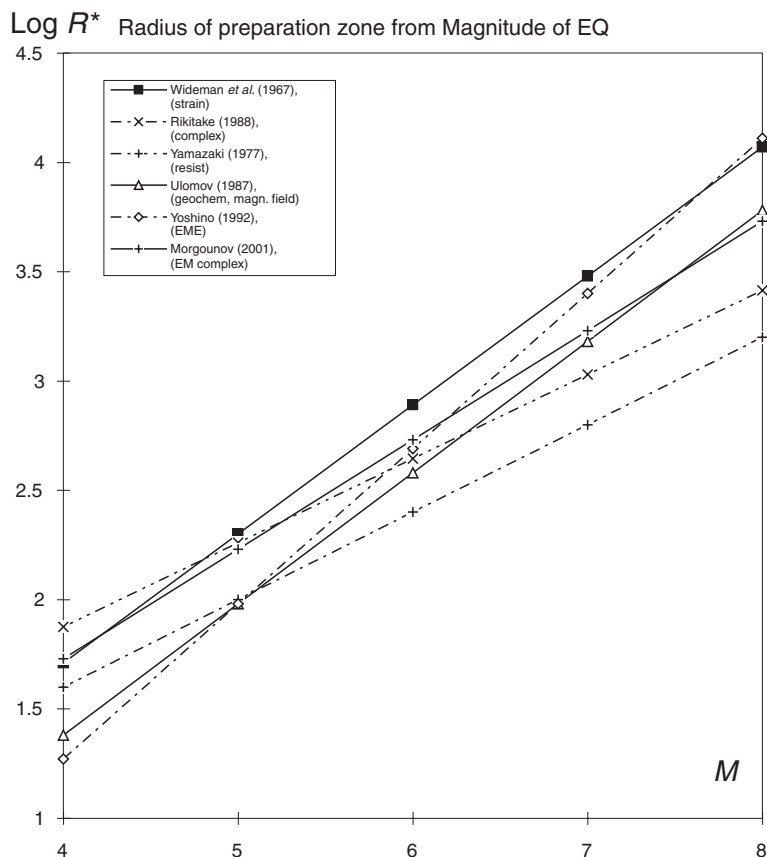


**Fig. 1.** Log  $R^*$ - $M$  relationships for precursory anomalies in various fields: strain steps (Wideman *et al.*, 1967); a summary of all available precursory data including strain, tilt, hydrogeochemical variations, microearthquakes, magnetic field, telluric currents, electromagnetic emission, and electrical resistivity (Rikitake, 1988); variometer data on the electrical resistivity (Yamazaki, 1977); geochemical and magnetic fields (Ulomov, 1987); electromagnetic emission (Yoshino *et al.*, 1992); and summarized electromagnetic data (Morgounov, 2001).

The solution of this old seismological enigma is beyond the scope of the present paper. Wideman's relation is plotted in the figure to demonstrate that this debatable relation gives distances of the same order of magnitude as the values obtained by other geophysical methods and apparently gives an upper limit of the precursor detection range. Wideman and Major estimated the amplitude of the observed strain at  $\varepsilon \sim 10^{-9}$ . According to Rikitake *et al.* (1985), such a deformation could be responsible for the generation of precursory anomalies in the resistance of the upper layers of the crust. This value was used in our calculations.

The results summarized in fig. 1 suggest that the variations in different parameters have the same origin, namely, the activation of the stress-strain state of the crust. Moreover, the similarity between the relations obtained for the so-called «propagating» fields, such as the electromagnetic emission (EME) in the Earth-ionosphere waveguide, and the «nonpropagating» fields (radon, electrical resistivity of rocks, groundwater level, etc.) is consistent with the idea that EM precursor sources (mechanical-to-electric energy converters) are located near the observation point in the skin-layer of the crust (Morgounov, 1985, 1991, 1995).

### 3. Short-term precursors and slip weakening

Earthquake precursors recorded on the Earth's surface are an indirect response of upper crust rocks to the strain evolution in the focal zone. Geological scales of the processes in the crust and its subcritical stress state require that the actual rheology of rocks, characterized by clearly expressed ductile properties, be taken into account.

At the final stage of the EQ nucleation process, the conditions in the focal zone are favorable for the development of tertiary creep characterized by well-pronounced self-regulation properties. An accelerated inelastic deformation in the focal volume, eventually results in a rupture whose dimension is controlled by its accumulated elastic energy ( $M$ ). Beginning from a certain time of plastic flow, strains and

strain rates in surface layers attain values that can be detected by geophysical instruments. Many authors considered slip weakening (or creep) as a possible mechanism of EQ generation (Benioff, 1951; Kranz and Scholz, 1977; Lockner and Byerlee, 1978). Rice and Rudnicki (1979) defined the precursor time as the duration of «self-maintained accelerating creep.»

It is evident that a real rock massif is not uniform. A fundamental property of the geophysical medium is the fact that it consists of a system of interacting heterogeneities (blocks and fractures) that constitute a strictly defined, discrete hierarchy of sizes of its elements. Due to the inadequate knowledge of the real crustal structure, unknown initial conditions of the deformation process, and the vague mechanism of EQ nucleation, an exact solution of the problem cannot be obtained at present. A deterministic description of such a medium is a problem unsolvable even statistically. Therefore, the medium should be characterized by generalized parameters in accordance with its scale factors (Sadovsky *et al.*, 1987). From this point of view, the heterogeneity of a rock massif does not seem to be an insuperable obstacle for the prognostic tasks.

Therefore, we use the assumption of a formally uniform half-space, and nominal strain value  $\varepsilon(t, r)$  keeping in mind that the strain value is a qualitative (measured on the order of magnitude) characteristic of the mosaic secondary response of local dislocations to the general *quasi*-elastic large-scale strain field. It meets the assumption of Benioff (1954) that elastic stresses can have a planetary scale. He substantiated the assumption by the regularity that the strongest earthquakes occur successively in different parts of the world (Turkey, Taiwan, and Greece: 1999; Algeria, Philippines, Taiwan, and Japan: May, 2003; etc.).

To describe phenomenologically the general relations between spatial and temporal scales of the nucleation, we make the following additional assumptions: a) creep mechanism; b) an  $r^{-3}$  attenuation of the stress-strain field; and c) calculations in terms of the normalized distance  $r_s/R^*$  for the purpose of obtaining general regularities applicable to EQs of various magnitudes. Given constant loading conditions ( $F =$

= const), the tertiary creep in rocks of the focal zone can be described by the power function of relative strain  $\varepsilon_f = \Delta l/l$

$$\varepsilon_f(t) = \Delta \varepsilon_f t^m + \varepsilon_f^0 \quad (3.1)$$

where  $\varepsilon_f(t)$  and  $\varepsilon_f^0$  are the current and initial strain values in the focal zone,  $t$  is time, and  $\Delta \varepsilon_f$  is the strain increment.

The deformed volume can be divided into two at least main parts (fig. 2): the nucleation (focal) zone of radius  $r_f$  in which the nonlinear creep process (governed by eq. (3.1)) develops and the surrounding rocks with *quasi*-elastic properties described by the equation

$$\varepsilon(r_1)/\varepsilon(r_2) = (r_2/r_1)^n \quad (3.2)$$

where  $r_1$  and  $r_2$  are the distances from the source to the points of measurement.

Taking into account the rheology of the real medium, the term «*quasi*-elastic surrounding medium» means here that a rock mass is able to transmit elastic stresses through the preparation region but possesses inelastic properties giving rise to surface precursors such as anomalous disturbances in electrical resistivity ( $\rho$ ), electromagnetic emission (EME), Acoustic Emission (AE), and others. Given constant loading conditions, the following notation is used below (fig. 3):  $t_f^e$  and  $t_s^e$ , the time of EQ in the source ( $f$ ) and at the surface ( $s$ );  $t_s^0$ , the onset time moment of the anomaly at the surface;  $t_f^0$ , the reference time of inelastic deformations in the source;  $\tau$ , the duration of the anomalous surface signal;  $T$ , the duration of the tertiary creep in the focal zone.

Thus, we have

$$\tau = t_s^e - t_s^0 \quad \text{and} \quad T = t_f^e - t_f^0. \quad (3.3)$$

Taking, in the first approximation,  $t_f^e = t_s^e$  and setting  $t_f^0 = 0$ , we obtain

$$\tau = T - t_s^0. \quad (3.4)$$

Also, the following notation is used below:  $\varepsilon_f^0$  and  $\varepsilon_f^e$ , initial and final strain values in the focal zone;  $\varepsilon_s^0$ , initial measurable strain (or strain-de-

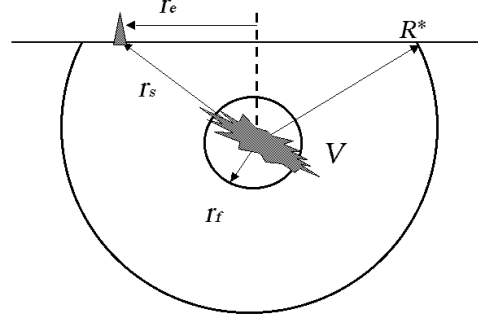


**Fig. 2.** A schematic layout of the earthquake nucleation zone:  $R^*$  is the ultimate distance of the preparation zone;  $r_f$  is the radius of the seismic source;  $r_e$  is the epicentral distance from the point of measurement;  $r_s$  is the hypocentral distance, and  $V$  is the source volume.

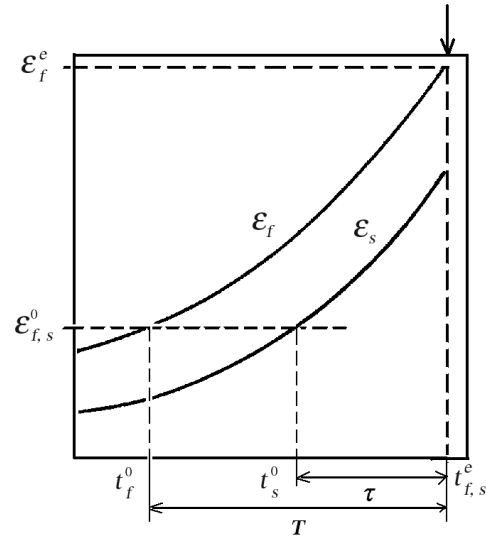


**Fig. 3.** Diagram illustrating the tertiary creep stage in the focal zone and at the Earth's surface. The following notation is used:  $t_f^e$  and  $t_s^e$ , time moments of an earthquake in the source ( $f$ ) and at the surface ( $s$ );  $t_s^0$ , time moment of the anomaly appearance at the surface;  $t_f^0$ , reference time of inelastic deformations in the source;  $\tau$ , duration of the anomalous surface signal;  $T$ , duration of the tertiary creep in the source zone;  $\varepsilon_f^0$  and  $\varepsilon_f^e$ , initial and final strain values in the source zone;  $\varepsilon_s^0$ , initial surface strain at which anomalies of geophysical parameters can be recorded;  $r_f$ , characteristic size of the source or the radius of the focal zone;  $r_s$ , hypocentral distance.

pendent parameter) at the surface;  $r_f$ , characteristic size of the source (the radius of the focal zone);  $r_s$ , hypocentral distance ( $r_s \geq r_f$ ).

We have  $\varepsilon_f^0 = \varepsilon_0$  at the time  $t = 0$  and  $\varepsilon_f^e = \Delta\varepsilon_f T^m + \varepsilon_0$  at  $t = T$ . Equation (3.1) yields

$$\varepsilon_f(t) = (\varepsilon_f^e - \varepsilon_0)(t/T)^m + \varepsilon_0. \quad (3.5)$$

According to (3.2) and (3.5), the strain at the surface ( $r = r_s$ ) at its initial time  $t = t_s^0$  is found from the conditions

$$\varepsilon_s^0(t_s^0, r_s) = [(\varepsilon_f^e - \varepsilon_0)(t_s^0/T)^m + \varepsilon_0](r_f/r_s)^n. \quad (3.6)$$

Then,

$$t_s^0 = \left\{ \left[ \varepsilon_s^0 (r_s/r_f)^n - \varepsilon_0 \right] T^m (\varepsilon_f^e - \varepsilon_0)^{-1} \right\}^{1/m}. \quad (3.7)$$

The substitution of (3.7) into (3.4) gives the following expression for the precursor duration  $\tau$  depending on the epicentral distance and EQ energy

$$\tau = T \left\{ 1 - \left[ \varepsilon_s^0 (r_s/r_f)^n - \varepsilon_0 \right] (\varepsilon_f^e - \varepsilon_0)^{-1} \right\}^{1/m}. \quad (3.8)$$

#### 4. Ultimate distance of precursor detection

The condition  $\tau = 0$  determines the ultimate distance  $r_s^{\max} = R^*$  at which the precursor can be detected. This condition and eq. (3.8) yield

$$R^* = r_f (\varepsilon_f^e / \varepsilon_s^0)^{1/n}. \quad (4.1)$$

The duration of inelastic deformation in the source is controlled by the initial strain  $\varepsilon_f^0$ , which depend on the sensitivity of the method in use and is actually a reference value. According to estimates given in (Yamazaki, 1977, 1983; Rikitake *et al.*, 1985), preseismic anomalies recorded by an electrical resistivity variometer comply with a surface strain not smaller than  $\varepsilon_s^0 = 10^{-9}$ . This value is taken here as an initial value of the tertiary creep process in the focal zone.

This provides certain constraints on the duration of the deformation process in the source. Taking into account the level of natural noise and the sensitivity of the method in use and

Dambara's (1966) way to evaluate the size of the focal zone  $r_f$ , we assume  $\varepsilon_f^0 = \varepsilon_s^0$ .

Numerical order-of-magnitude estimates can be made as follows. According to various authors (in particular, Rikitake, 1976), the rupture of rocks occurs at  $\varepsilon_f^e \sim 10^{-4}$ . Equation (4.1) at  $n = 3$  gives  $R^*/r_f \sim 50$ . The source size  $r_f$  being strongly dependent on the magnitude  $M$ , numerical estimates of  $r_f$  can be derived from the formula (Dambara, 1966)

$$r_f = (10^{0.5M-2.27} \text{ km}). \quad (4.2)$$

Using the statistics of data for geophysical precursors of 13 types, Rikitake (1988) obtained a general empirical formula relating the maximum distances  $D$  (*i.e.* radius of the earthquake preparation zone,  $D = R^*$ ) within which the precursors are detectable and the earthquake magnitude:  $M = -0.87 + 2.6 \log D$ . Dividing this relation by eq. (4.2), we obtain  $R^*/r_f = 138, 106, 81, \text{ and } 62$  for the respective magnitudes  $M = 4, 5, 6, \text{ and } 7$ , with the average value being  $R^*/r_f \sim 96$  for  $M = 4-7$ . Consequently, the maximum range of the precursor detection can be approximately hundred times as large as the source size.

Data of Yamazaki's variometer (Rikitake and Yamazaki, 1985) provide the following estimates for the ultimate normalized distances of a short-term precursor (see no. 5, 8, and 21 in table I, and eq. (4.2)):  $r_s/r_f = 85.7, 92.7 \text{ and } 86.5$ . Therefore, the estimate  $R^*/r_f \sim 50$ , obtained above for  $\varepsilon_f^e \sim 10^{-4}$  and  $\varepsilon_s^0 \sim 10^{-9}$ , is inconsistent with the experimental data. Thus, the value  $R^*/r_f \sim 10^2$  is more adequate to *in situ* measurements

$$R^*/r_f = (\varepsilon_f^e / \varepsilon_s^0)^{1/3} \sim 10^2. \quad (4.3)$$

Hence, we have  $(\varepsilon_f^e / \varepsilon_s^0) \sim 10^6$ . This can increase the known estimates of the *in situ* ultimate strain to the value  $\varepsilon_f^e \sim 10^{-3}$ , which is consistent with data of direct measurements of the breaking strain in rocks under laboratory conditions (Kasahara, 1981). (Note that the value  $R^*/r_f \sim 10^2$  with  $\varepsilon_f^e \sim 10^{-4}$  is consistent with  $\varepsilon_s^0 \sim 10^{-10}$ ). Thus, the value  $R^*/r_f \sim 10^2$  complies with data of the *in situ* resistivity observations by Yamazaki. Then, considering eqs. (4.2) and (4.3),

**Table I.** 30 earthquakes that were preceded by preseismic resistivity variations (Rikitake and Yamazaki, 1985) and their calculated parameters. Note:  $M$  – magnitude;  $h$  – depth;  $r_e$  – epicentral distance;  $r_s$  – hypocentral distance;  $\tau$  – precursor duration;  $R^*$  – maximum size (radius) of the preparation zone;  $r_f$  – characteristic size (radius) of the focal zone;  $r_s/R^*$  – normalized hypocentral distance.

No.	Data	$M$	$h$ (km)	$r_e$ (km)	$r_s$ (km)	$\tau$ (hour)	$R^*$ (km)	$r_s/R^*$	$r_f$ (km)
1	16.05.1968	7.9	0	935	935	2	4786	0.195	47.9
2	01.07.1968	6.1	50	127	136	3-4 h 45 min	603	0.226	06.0
3	12.08.1969	7.8	30	1094	1094	4	4266	0.330	42.7
4	09.09.1969	6.6	0	320	320	2 h 15 min	1072	0.299	10.7
5	06.01.1971	5.5	40	256	259	0.5	302	0.858	03.0
6	23.07.1971	5.3	10	100	100	5	240	0.417	02.4
7	02.08.1971	7.0	60	1004	1005	7	1698	0.592	01.7
8	12.08.1971	4.8	60	110	125	0.5	135	0.927	01.35
9	06.10.1972	5.5	30	174	177	0.5	302	0.586	03.02
10	04.12.1972	7.2	50	337	341	2-7	2138	0.159	21.4
11	27.03.1973	4.9	60	66	89	3	151	0.588	01.51
12	30.09.1973	5.9	50	147	155	1	479	0.324	04.79
13	03.03.1974	6.1	60	160	171	3	603	0.284	06.03
14	09.05.1974	6.9	10	144	144	4	1514	0.095	15.14
15	27.09.1974	6.4	60	311	317	2-10	851	0.372	08.51
16	16.10.1974	6.1	40	215	219	2	603	0.363	06.03
17	30.10.1974	7.6	420	673	792	4-9	3388	0.234	33.90
18	02.04.1975	5.8	40	194	198	5-11	427	0.464	04.27
19	20.02.1978	6.7	50	461	464	3.5	1202	0.386	12.00
20	07.04.1978	6.1	30	160	163	1	603	0.271	06.03
21	13.08.1978	4.7	80	67	104	1 h 15 min	120	0.865	01.20
22	03.12.1978	5.4	20	50	54	5.5	269	0.201	02.69
23	11.07.1979	5.9	40	223	227	1	479	0.474	04.79
24	28.10.1979	5.5	90	104	138	6	302	0.457	03.02
25	12.03.1980	5.6	80	85	117	1	339	0.345	03.39
26	08.05.1980	5.7	60	104	120	6 h 45 min	380	0.316	03.80
27	29.06.1980	6.7	10	45	46	0.5-5	1202	0.038	12.00
28	25.09.1980	6.1	80	69	106	1	603	0.176	06.03
29	21.02.1982	6.7	0	230	230	8	1202	0.191	12.00
30	23.07.1982	7.0	10	241	241	3.5	1698	0.142	17.00



the following formula can be obtained for estimating the ultimate radius of the strain sensitivity (preparation) zone (fig. 1):

$$R^* = (10^{0.5M-0.27} \text{ km}). \quad (4.4)$$

For example, eq. (4.4) yields  $R^* \sim 1700$  km for  $M = 7$  and  $R^* \sim 5400$  km for  $M = 8$ ; *i.e.* the strain-sensitivity zone can extend over considerable distances from the epicenter. This approach explains, in particular, the long-range effects of strain-related precursors, including «strange» (in terms of Rikitake and Yamazaki, 1985) precursors in rocks recorded at epicentral distances longer than  $10^3$  km.

The stereotypes associated with the property of EM waves to propagate over large distances dominated the early model concepts of the EM precursor range. However, the examples presented above show that the waveguide propagation model of an EM signal fails to account for the long-range effect of strain-related resistivity precursors recorded at epicentral distances of up to a thousand kilometers, and the same is true of geochemical, hydrodynamic, and other precursory phenomena (Lomnitz and Lomnitz, 1978; Fleischer, 1981; Warwick *et al.*, 1982; Tramutoli *et al.*, 2001).

In particular, the preparation zone radius of the Chilean earthquake of 1960 ( $M = 8.5$ ) is estimated at  $R^* \sim 9550$  km according to (4.4). This agrees with the data of Warwick *et al.*

(1982), who recorded radiowave precursors of this earthquake at distances of up to  $10^4$  km (the formula of Rikitake (1988) gives  $R^* \sim 4075$  km for this magnitude, fig. 1).

Note once more that Tomaschek (1955) reported special tilts of about 0.1 s that were recorded in Japan at an epicentral distance of  $\sim 1800$  km 20 h before the Taiwan earthquake of  $M = 7$ . In this case, the relation (4.4) gives a similar value for the ultimate radius of preparation zone ( $\sim 1700$  km). Is this coincidence accidental? The answer requires additional *in situ* data in order to perform independent detailed analysis.

Such EQ parameters as the magnitude, depth and epicentral distance allow the estimation of the nominal strain value at an observation point. At the epicentral distance  $r_s$ , eqs. (4.1) and (4.2) yield ( $\varepsilon_f^e = 10^{-3}$ )

$$\varepsilon_s = (10^{1.5M-9.81}) r_s^{-3}. \quad (4.5)$$

Table II presents the values  $R^*$  and  $\varepsilon_s$  estimated by eqs. (4.4) and (4.5). Rikitake (1976) reported preseismic strain anomalies that enabled such estimation (case no. 1, 2, and 3 in table II). Case no. 4 illustrates the estimated strain value  $\varepsilon_s$  at the observation point and the value of  $R^*$  in the case of the preseismic EM event recorded by Warwick *et al.* (1982) at five US stations before the Great Chilean earthquake of May 22, 1960 at distances of up to 10 000 km. Event no.

**Table II.** Examples of calculated values  $\varepsilon_s$ ,  $R^*$ , and  $r_s/R^*$  in comparison with parameters of some earthquakes that were preceded by precursory variations.

No.	$M$	$\Delta$ km	$h$ km	$\varepsilon$ ( <i>in situ</i> )	$\varepsilon$ (calcul.)	$R^*$ km	$r_s/R^*$	References
1	7.0	94	70	$2.5 \cdot 10^{-6}$	$3.0 \cdot 10^{-6}$	1700	0.068	Rikitake (1976)
2	6.0	250	N	$4.0 \cdot 10^{-8}$	$1.0 \cdot 10^{-8}$	537	0.46	Rikitake (1976)
3	3.0	5	N	$3.0 \cdot 10^{-8}$	$3.9 \cdot 10^{-8}$	17	0.29	Rikitake (1976)
4	8.5	10 000	N		$0.9 \cdot 10^{-9}$	9549	$\sim 1$	Warwick (1982)
5	6.6	368	16		$1.7 \cdot 10^{-8}$	1071	0.34	Eftaxias (2002)
6	5.9	359	N		$2.0 \cdot 10^{-9}$	478	0.75	Eftaxias (2002)
7	6.5	192	N		$1.2 \cdot 10^{-7}$	955	0.20	Eftaxias (2002)

5, 6 and 7 represent a few recent EQs in Greece, including the destructive earthquake of September 7, 1999 ( $M = 5.9$ ) in Athens. A distinct pre-seismic EME signal was recorded by Eftaxias *et al.* (2002) at a distance of  $\sim 370$  km (event no. 6 is yielded a nearly ultimate value of the normalized radius,  $r_s/R^* = 0.75$ ).

Table II shows that all precursors (including those recorded at great distances) were observed within the preparation zone of radius  $R^*$  eq. (4.4). Obviously, the uncertainty of the precursor detection increases with distances approaching the ultimate value (only 10% of all the events, table I). It is natural that more reliable detection of precursors can be expected

closer to the epicentral zone where the strain values are higher. For example, in the case of  $\varepsilon \sim 10^{-6}$  the «effective» radius of the preparation zone  $R_{\text{eff}}^*$  is determined by the expression

$$R_{\text{eff}}^* = (10^{0.5 M - 1.27} \text{ km}). \quad (4.6)$$

### 5. Creep duration and normalized precursor time

Undoubtedly, the determination of main invariant relationships in the space-time distribution of short-term precursors is a key point in solving the prediction problem. Published data

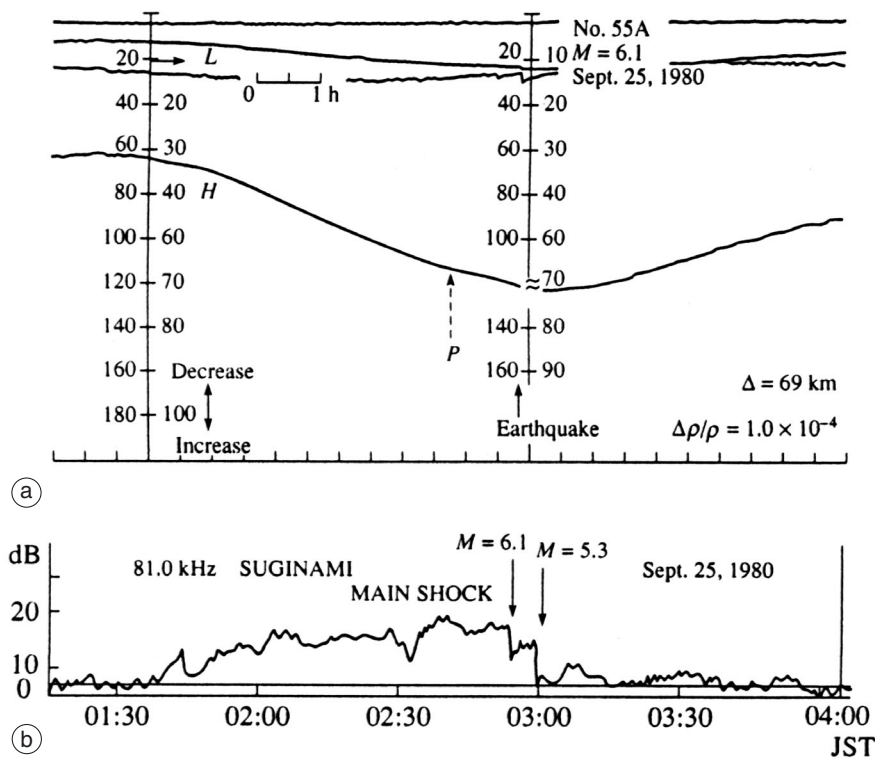


**Fig. 4a,b.** Synchronous development of anomalous disturbances in the variometer record of electrical resistivity and EME in Japan at points 50 km apart one from the other and 70 km apart from the epicenter. a) Example of an electrical resistivity variation before an  $M = 6.1$  earthquake (Kanto area) at the epicentral distance  $r_e = 69$  km (September 25, 1980). The symbol «P» and the dotted arrow indicate the onset of the anomaly. The solid arrow indicates the onset moment of the earthquake. The time scale is shown in the top left corner (Yamazaki, 1983). b) EME level at a frequency of 81 kHz from observations at the Suginami seismic station near Tokyo before the same earthquake (Gokhberg *et al.*, 1982).

are mainly episodic measurements related to individual seismic events. In this context, well-documented long-term data recorded by Yamazaki's variometer ( $\rho$ ) over 30 years (1968-1998) provide a good opportunity for testing the model described above.

Yamazaki (1977, 1983) subdivided seismic anomalies into preseismic and coseismic types. The data on preseismic anomalies are still the subject of vivid discussions or mistrust. Yamazaki (1977, 1983) and Rikitake and Yamazaki (1985) presented 14-year data (1968-1982) in the form of records of preseismic  $\rho$  anomalies for 30 EQs with magnitudes of 4.7-7.9 that occurred in the region; they also presented the duration of the anomalies, their relative amplitudes, epicentral distances, and focal depths.

Yoshino *et al.* (1998) questioned the reliability of these data because, in their opinion, the successive records of 1982-1997 revealed no precursors. This obvious contradiction requires an explanation.

Undoubtedly, the preseismic anomaly presented in fig. 4a (Yamazaki, 1983) is debatable from the standpoint of an independent expert. However, it is important to note that this particular «questionable» anomaly recorded at the Aburatsubo Observatory (Yamazaki, 1983) coincides in the times of arrival, duration, and completion with the EME anomaly independently recorded at the Suginami Observatory (Yoshino *et al.*, 1992) before the same seismic event (fig. 4b). Comparative analysis of published data reveals several coincidences of this kind.

After the first EME measurements made by Morgounov, Yoshino and Tomizawa in 1980 in Japan (Gokhberg *et al.*, 1982), Yoshino *et al.* (1992) published the statistics of EME precursors over the period from 1985 through 1990. The joint analysis of data published in Yoshino *et al.* (1992, 1998) showed that at least ten anomalous resistivity disturbances recorded in this period coincided in time with EME precursors (Yoshino *et al.*, 1992), and these coincidences cannot be considered accidental. In other words, the resistivity anomalies reported in Yamazaki (1977, 1983), Rikitake and Yamazaki (1985) and Rikitake (1988) are actually precursory anomalies due to the earthquake nucleation process and deserve a more detailed analysis.

Similar to precursory anomalies of other types, the duration of  $\rho$  precursors is invariably irregular as a function of the epicentral distance. Figure 5a illustrates this with 30 cases recorded in 14 years (see table I) (Rikitake *et al.*, 1985). In order to estimate the minimum duration of the rock failure process in the focal zone, only the anomalies that developed monotonically prior to an EQ were chosen from table I.

By analogy with the notion of «canonical» creep, which is a deformation process gradually developing under a constant load, we introduce the term «canonical» for a precursor that continuously develops until earthquake onset. Nearly 80% of all cases from table I meet this condition. In six cases (20%), anomalous disturbances ended before the earthquake onset (no. 7, 10, 15, 17, 18, and 26 in table I). These cases are shown as stars in fig. 5a.

As is evident from the diagram (fig. 5b) showing the distribution of the duration times of «canonical» precursors as a function of the hypocentral distance  $r_s$  normalized to the radius of preparation zone  $R^*$  (eq. (4.4)), the chaotic set of points in fig. 5a is transformed into a group of points bounded by the straight line fitting the maximum duration values  $\tau_{\max}$  of canonical precursors in  $\rho$  recorded at various normalized distances  $r_s/R^*$  from epicenter (fig. 5b).

These maximum values are of particular interest. The precursor durations  $\tau$  that are smaller than the critical value  $\tau_{\max}$  (the points below the straight line in fig. 5b) can be naturally interpreted in terms of an indistinct, inadequate manifestation of precursors due to the mosaic space-time pattern of the deformations, nonuniformity of the stress field, varying strain sensitivity at the observation point, or specific features of a particular earthquake mechanism.

The regression line approximating the maximum values  $\tau_{\max}$  (no. 6, 21, 24, and 29 in table I; open circles in fig. 5b) is  $\tau = 9.83 - 9.88 (r_s/R^*)$  with  $\lambda^2 = 0.96$ . Within a reasonable accuracy, this gives the following empirical formula:

$$\tau \cong T_0(1 - r_s/R^*) \quad (5.1)$$

where  $T_0 \sim 10$  h.

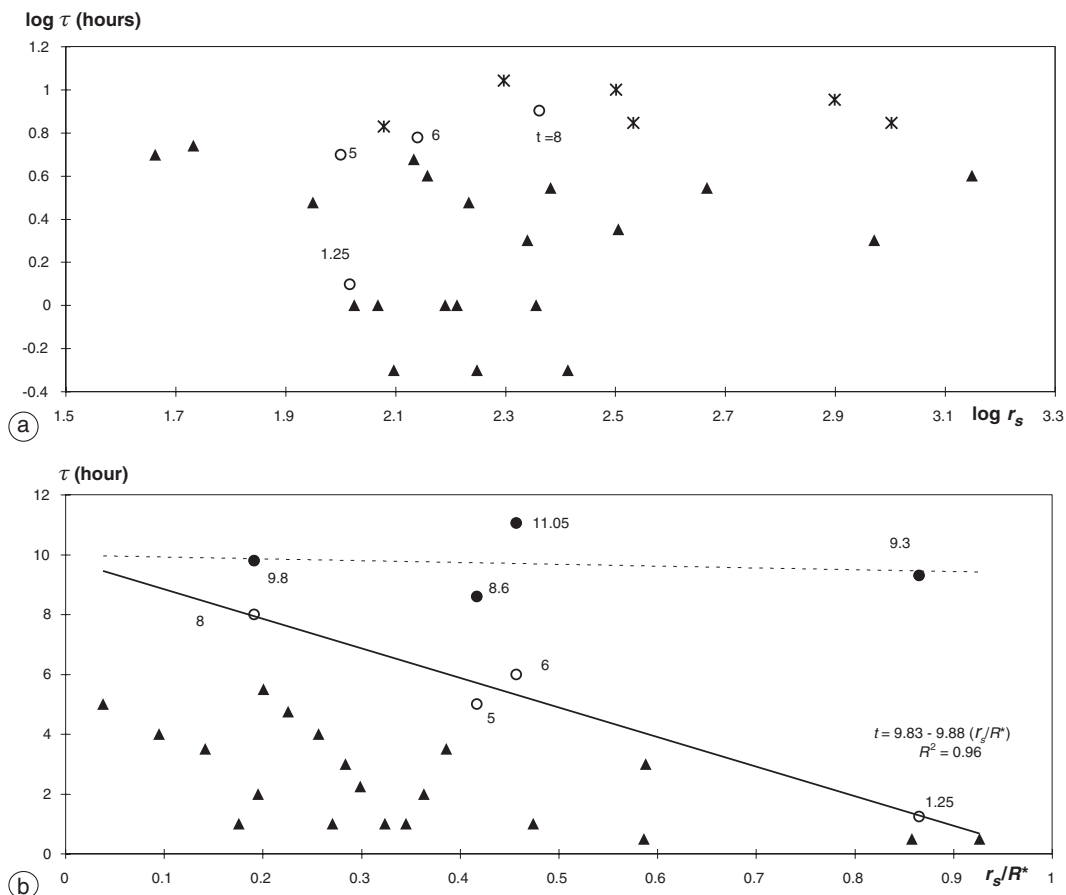


**Fig. 5a,b.** a) Time of the electrical resistivity precursor ( $\log \tau$ ) versus the logarithm of the hypocentral distance ( $\log r_s$ ) (Rikitake and Yamazaki 1985). The triangles and circles are precursors that continuously developed until the earthquake onset (*i.e.* «canonical» cases). The stars are precursors that terminated before an earthquake (no. 7, 10, 15, 17, 18, and 26). The circles indicate the events with  $\tau_{\max}$  in terms of the normalized distance  $r_s/R^*$ . The numbers near circles indicate the duration of the precursors in hours. b) Duration of a precursor and a failure process in the focal zone as a function of the hypocentral distance normalized to the size of preparation zone  $R^*$ . The triangles and open circles indicate the «canonical» cases (see table I). Open circles (no. 6, 21, 24, and 29) indicate the events with  $\tau_{\max}$  estimated in terms of the normalized distance  $r_s/R^*$ . Solid circles are duration times of the fracture process in the source calculated from eq. (5.1) for the events with the precursors shown as open circles.

Thus, one can evaluate empirically the duration of slip stage of rocks in the source. When distance to the focal zone decreases, *i.e.* at  $r_s \rightarrow r_f$ , we have  $\tau \rightarrow T_0$ . Data by Yamazaki (1977, 1983) yield  $T_0 = 9.885 \approx 10$  h as an empirical estimate of the ductile failure duration in the source. As

seen from fig. 5b, four precursory events (only  $\sim 13\%$  of all cases) were observed in the immediate vicinity of the normalized ultimate epicentral distances.

Empirical formula (5.1) complies with theoretical formula (3.8). Since  $\varepsilon_f^e/\varepsilon_s^0 \approx 10^5 - 10^6 \gg 1$

and  $m = n = 3$ , we have  $(r_s / r_f)^3 \gg 1$ , and this agrees with the *in situ* observed distances for which  $r_s / r_f > 2-3$ . Substitution of these values into (3.8) gives formula (5.1).

The agreement between theoretical formula (3.8) and empirical formula (5.1) suggests that the process of tertiary creep in form (3.1) can be considered, to a first approximation, as a mechanism responsible for the fracture of the source rock mass. It also confirms the validity of Yamazaki's precursors (Yamazaki, 1983; Rikitake *et al.*, 1985).

Equations (3.8) and (5.1) can be transformed into the form suitable for estimating the minimum time of the ductile failure  $T_0$  in the source ( $r_s \neq R^*$ )

$$T = \tau (1 - r_s / R^*)^{-1}. \quad (5.2)$$

For cases 6, 21, 24, and 29 (table I; solid circles in fig. 5b), we obtain  $T_0 = 9.8, 8.6, 11,$  and  $9.3$ , respectively.

The dotted line in fig. 5b is the regression line approximating the  $T_0$  values for  $\tau_{\max}$  at different normalized distances. This regression line indicates that the rate of creep at its final stage apparently has a limiting value ( $T_0 \sim 10$  h) that is independent of the earthquake magnitude (at least in the range  $M = 4.7-6.7$  of the cases 6, 21, 24, and 29).

Naturally, the  $T_0$  value is determined by the onset time  $t_f^0$  of the plastic deformation that in turn depends on the sensitivity of the method  $\varepsilon_s^0$ . Therefore, the duration of the fracture monitoring can generally be extended with the use of more perfect instrumentation. It is obvious that there exists a natural threshold of detection of seismogenic anomalies due to natural noises (tides, temperature, local geodynamic processes, etc.).

## 6. Discussion

The agreement between the empirical (5.1) and theoretical (3.8) relations is remarkable and suggests that the initial assumption on the creep mechanism can be consistent with the natural process, at least, as regards the events considered. The conclusion on the invariance of  $T_0$

complies with the known evidence on the smallness of the scale factor during plastic deformations (McClintock, 1976). Studying the scale factor in rocks under laboratory conditions, Mogi (1988) came to the same conclusion that the dimension effect on the strength of rock samples is insignificant.

Several authors noted that, with the energies of earthquakes covering a range of a few orders of magnitude, the amplitudes of variations in precursors vary insignificantly, and this supporting the fundamental hypothesis of Tsuboi (1956), according to which a rock volume is characterized by an ultimate strength, implying that the ratio of elastic energy to the seismic source volume is a global characteristic and, in a first approximation, is independent of rock properties. The inference of the present work stating that  $T_0$  is invariant, *i.e.* that the minimum time of the creep-type failure (under a *quasi*-constant load) in the seismic source (eq. (3.7)) is independent of the magnitude ( $M$ ), is also consistent with the Tsuboi hypothesis and extends the latter to the duration of the ductile failure stage.

Within the framework of the tertiary creep under constant load conditions, the strain rate increases up to the fracture value. In practice, an earthquake can occur during the period of relatively smooth development of an anomaly, with no intensity peaks preceding the main shock. Moreover, many earthquakes occur during the decay period of a bay-like anomalous disturbance or after its completion, during the so-called quiescence period of the signal. In this case, the usual model of avalanche creep under a constant load cannot serve as a direct analogy of the fracture development.

The uniaxial loading of a sample under laboratory conditions differs from *in situ* conditions in that the load applied to an *in situ* deformed rock mass does not remain constant during the process of plastic flow but decreases because due to considerable creep strain and the fact that this process proceeds in the environment of surrounding rocks contributing to the load redistribution.

The mechanism of creep failure under load relaxation conditions provides an explanation for various precursory signatures, as well as

signal-quiescence earthquakes and precursors of the oscillatory type. The deceleration of the failure process, *i.e.* an increase in the precursor duration (several hours, a few days) and signal instability degree, can be interpreted in terms of the mechanism of stress relaxation during the deformation of the focal zone volume (the relaxation creep model: Morgounov, 2001). Events 7, 10, 15, 17, 18, and 26 (see table I), which have been excluded from the analysis under the  $F=\text{const}$  condition, have features characteristic of the failure of the relaxation type. The generation of anomalous disturbances unaccompanied by an earthquake (silent, or slow earthquakes) seems to be a natural element of the nucleation process (false alarm) and can be regarded as a consequence of the relaxation creep mechanism. The quiescent phase of relaxation creep could be the reason why preseismic anomalies could not be detected when measurements were made immediately (a few minutes or hours) before a shock.

The creep mechanism is effective under conditions of either pure compression (extension) or pure shear (Benioff, 1951). Therefore, this model can be applied to the results obtained in seismically active regions dominated by shear deformations (the San Andreas and Anatolian faults), subduction zones (Kuril-Kamchatka and Japan islands), or continental areas of China subjected to compression. The value  $T_0 \sim 10$  h was obtained using data from the subduction zone of Japan. Analysis of experimental data from other regions can provide constraints on the variability of this value.

## 7. Conclusions

Johnston and Linder (2002) noted that observations of crustal strain in high sensitivity zones near large earthquakes during the final stages before the rupture are unfortunately rare, and the knowledge of the timescale and mechanics of failure is therefore limited. This is largely due to a relatively low recurrence of earthquakes and sparseness of adequate instrumental networks.

The discrepancy between the results of the strain measurements, and the other geophysical

disciplines, and expected theoretical values suggests that blocks can concentrate regional stresses at a relatively small portion of their perimeters. Then, the average stress on block boundaries can be relatively low. Thus, the observation of aseismic deformation preceding earthquakes is consistent with the block tectonics (Leary *et al.*, 1984). Such secondary local mosaic effects could explain why direct stress measurements at a given point have a low probability to detect preseismic anomalies. In other words, this probability depends on the number of stations and/or the detection of a sensitive point of stress concentration.

From this point of view, taking into account elements of SOC phenomena, the problem of the epicenter location seems to be more unreliable than the determination of the time interval (from the similarity of temporal scales) and the magnitude (from spatial scales) of the pending shock. Exact calculations of the strain of an impending earthquake in such a medium are problematic. Nevertheless, the calculations in a formal uniform half-space can be useful for the qualitative estimation of the possible (maximal) secondary mosaic response of a fractal rock mass near the surface to the seismogenic strain evolution in the nucleation volume.

Thus, the main problem is not the absence of precursory anomalies (they do exist!) but the nonadequate response of a fractal crust to the source fracture process. Does this mean the insolvability of the prediction task? The response of local dislocations to a field of a larger scale reflects, to an extent, the general nucleation creep process in the source. Under favorable conditions, the measurements mirror the nucleation process in the source that resulted in successful predictions in the past (Raleygh *et al.*, 1977; Hui *et al.*, 1997).

A considerable increase in the strain rate before the failure significantly raises the signal-to-noise ratio, which is beneficial to the identification of short-lived precursors and provides an opportunity to explain published data on preseismic anomalous disturbances recorded at ultimate (teleseismic) distances during strong earthquakes. The relative (normalized) epicentral distance is beneficial to the comparison of geometrically similar earthquakes of different mag-

nitudes. This concept makes it possible to analyze a «telesismic equivalent» of seismic events of a lower energy. For example, the ultimate radius of an  $M \sim 5.0$  preparation zone is approximately  $R^* = 150$  km (eq. (4.4)), *i.e.* the distance 150 km for an  $M = 5$  event is equivalent to the telesismic distance  $R^* = 5400$  km of a strong,  $M = 8.0$  EQ. In both cases  $r/R^* \sim 1$ . Thus, the phenomena of teleseismic precursory effects does not seem to be abnormal and can be measured in exceptional cases under favorable conditions (Tomaschek, 1955; Wideman *et al.*, 1967; Lomnitz *et al.*, 1978; Warwick *et al.*, 1982; Yamazaki, 1983; and others).

The real strain field is a superposition of the complicated strain field of the source and heterogeneous geological structures and topography, giving rise to an intricate pattern of stress-strain state controlled by fault structures. The satellite image of thermal infrared anomalies demonstrated by Tramutoli *et al.* (2001) illustrates this natural mosaic distribution of precursors associated with the strain field. These patterns are the possible reason strain-metering instruments fail to record short-lived precursors at a given point, and why more «integral» methods (like EME) are more efficient than point-wise strain measurements.

Returning to the question whether SOC is an insurmountable obstacle for EQ prediction, it is appropriate to note the conclusion by Sykes *et al.*, (1999) that this issue does not depend on the SOC nature of seismicity. It depends on whether there exists a precursory phase of instability that can be reliably detected from instrumental observations.

Numerous studies performed in various countries, including the positive experience of a «negative results», is a good reason for reserved optimism with respect to future research.

### Acknowledgements

The author would like to express sincere thanks to M.J.S. Johnston for helpful discussions regarding the problem of the creep-strain measurements and V. Lapenna for reviewing the manuscript and valuable comments.

### REFERENCES

- ABERCROMBIE, R.E., D.C. AGNEW and F.K. WYATT (1995): Testing a model of earthquake nucleation, *Bull. Seismol. Soc. Am.*, **85** (6), 1873-1878.
- BAK, P., C. TANG and K. WIESENFIELD (1988): Self-organized criticality, *Phys. Rev. A*, **38**, 364-374.
- BENIOFF, H. (1951): Earthquake and rock creep, *Bull. Seismol. Soc. Am.*, **41** (1), pp. 30-62.
- BENIOFF, H. (1954): Evidence for world strain readjustment following the Kamtshatka earthquake of November 4, 1952, *Bull. Seismol. Soc. Am.*, **44** (3), 543-.
- BEN-ZION, Y., T.L. HENYAY, P.C. LEARY and S.P. LUND (1990): Observations and implications of water well and creepmeter anomalies in the Mojave segment of the San Andreas Fault Zone, *Bull. Seismol. Soc. Am.*, **80** (6), 1661-1676.
- BERGER, I. (1973): Application of laser techniques to geodesy and geophysics, in *Advances in Geophysics*, edited by H.E. LANDSBERG and J. VAN MIEGHEM (Academic Press, New York), vol. 16, 1-56.
- BILHAM, R.G. and R.J. BEAVAN (1979): Strain and tilts on crustal blocks, *Tectonophysics*, **52**, 123-138.
- DAMBARA, T. (1966): Vertical movements of the earth's crust in relation to the Matsushiro earthquake, *J. Geod. Soc. Jpn.*, **12**, 18-25.
- DIETERICH, J.H. (1992): Earthquake nucleation on faults with rate- and state-dependent strength, *Tectonophysics*, **211**, 115-134.
- DODGE, D.A., G.C. BEROZA and W.L. ELLSWORTH (1996): Detailed observations of Valifornia foreshock sequences: implications for the earthquake initiation process, *J. Geophys. Res.*, **101** (B10), 22371-22392.
- EFTAXIAS, K., P. KAPIRIS, E.J. DOLOGLOU, J. KOPANAS, N. BOGRIS, G. ANTONOPOULOS, A. PERATZAKIS and V. HADJICONTIS (2002): EM anomalies before the Kozani earthquake: a study of their behavior through laboratory experiments, *Geophys. Res. Lett.*, **29** (8), 69,1-69,4.
- FLEISCHER, R.L. (1981): Dislocation model for radon response to distant earthquakes, *Geophys. Res. Lett.*, **8** (5), 477-480.
- FRASER-SMITH, A.C., A. BERNANDI, P.R. MC-GILL, M.E. LADD, R.A. HELLIWELL and O.G. VILLARD JR. (1990): Low-frequency magnetic field measurements near the epicenter of the  $M_s$  7.1 Loma Prieta earthquake, *Geophys. Res. Lett.*, **17** (9), 1465-1468.
- HARRIS, R.A. (1998): Introduction to special section: stress triggers, stress shadows, and amplification for seismic hazard, *J. Geophys. Res.*, **103** (B10), 24347-24358.
- HUI, LI and R. KERR (1997): Warning precede Chinese temblors, *Science*, **276** (5312), p. 526.
- GELLER, R.J. (1997): Earthquakes: thinking about the unpredictable, *EOS, Trans. Am. Geophys. Union*, **78**, 63-67.
- GOKHBERG, M.B., V.A. MORGOUNOV, T. YOSHINO and I. TOMIZAWA (1982): Experimental measurements of electromagnetic emissions possibly related to earthquakes in Japan, *J. Geophys. Res.*, **82**, 7824-7888.
- JOHNSTON, M.J.S. and A.T. LINDER (2002): Implications of crustal strain during conventional, slow, and silent earthquakes, *Int. Handb. Earthquake Eng. Seismol.*, **81A**, 589-605.
- JOHNSTON, M.J.S., A.T. LINDER and D.C. AGNEW (1994):

- Continuous borehole strain in the San Andreas Fault Zone before, during, and after the 28 June 1992,  $M_w$  7.3 Landers, California, Earthquake, *Bull. Seismol. Soc. Am.*, **84** (3), 799-805.
- KASAHARA, K. (1981): *Earthquake Mechanics* (Cambridge Earth Science Series, Cambridge Univ. Press), pp. 250.
- KRANZ, R.L. and C.H. SCHOLZ (1977): Critical dilatant volume of rocks at the onset of tertiary creep, *Geophys. Res.*, **82** (30), 4893-4898.
- LEARY, P.S. and P.E. MALIN (1984): Ground deformation events preceding Homestead Valley earthquakes, *Bull. Seismol. Soc. Am.*, **74** (5), 1799-1817.
- LOCKNER, D. and J. BYERLEE (1978): Development of fracture planes during creep in granite, in *2nd Conference on Acoustic Emission, «Microseismic Activity in Geologic Structures and Materials»*, Pennsylvania State University, 11-25.
- LOMNITZ, C. and L. LOMNITZ (1978): Tangshan 1976: a case history in earthquake prediction, *Nature*, **171**, 109-111.
- MCCLINTOCK, F.A. (1976): *Engineering Foundations and Interactions with the External Environment* (Mir, Moscow), pp. 262.
- MELONI, A., D. PATELLA, F. VALLIANATOS and B. ZOLESI (2001a): 2nd International Workshop Magnetic Electric and Electromagnetic Methods in Seismology and Volcanology, Chania, Greece, September 22-24, 1999, *Ann. Geofis.*, **44** (2), pp. 297.
- MELONI, A., D. DI MAURO, G. MELE, P. PALANGIO, T. ERNST, and R. TEISSEYRE (2001b): Evolution of magnetotelluric, total magnetic field, and VLF field parameters in Central Italy: relations to local seismic activity, *Ann. Geofis.*, **44** (2), 383-394.
- MOGI, K. (1981): Earthquake prediction program in Japan, in *Earthquake Prediction: an International Review*, edited by D.W. SIMPSON and P.G. RICHARDS (AGU, Washington, D.C.), Maurice Ewing Ser. 4, 635-666.
- MOGI, K. (1988): *Earthquake Prediction* (Tokyo, Academic), pp. 382.
- MORGOUNOV, V.A. (1985): Electromagnetic emission prior to seismic activity, *Izv. Akad. Nauk SSSR, Fiz. Zemli*, **3**, 220-226.
- MORGOUNOV, V.A. (1991): Creep processes in geodynamics, *Dokl. Akad. Nauk*, **317** (3), 1347-1352.
- MORGOUNOV, V.A. (1995): Tertiary creep in focal zone and immediate time earthquake prediction, *J. Earthquake Pred. Res.*, **5** (2), 155-181.
- MORGOUNOV, V.A. (2001): Relaxation creep model of impending earthquake, *Ann. Geofis.*, **44** (2), 369-381.
- MOUNT, V.S. and J. SUPPE (1992): Present-day orientations adjacent to active strike-slip faults: California and Sumatra, *J. Geophys. Res.*, **97**, 11995-12013.
- OHNAKA, M. (1993): Critical size of the nucleation zone of earthquake rupture inferred from immediate foreshock activity, *J. Phys. Earth*, **41**, 45-56.
- OKI, Y. and S. HIRAGA (1988): Groundwater monitoring for earthquake prediction by an Amateur Network in Japan, *Pure Appl. Geophys.*, **126** (2-4), 211-240.
- O'NEIL, J.R. and C. KING (1981): Variations in stable-isotope ratios of ground waters in seismically active regions of California, *Geophys. Res. Lett.*, **8** (5), 429-432.
- PRESS, F. (1965): Displacements, strains, and tilts at teleseismic distances, *J. Geophys. Res.*, **70** (10), 2395-2412.
- RALEYGH, B., G. BENNET, H. CREYG, P. MOLNAR, T. HANKS, A. NUR, F. WU, J. SAVAGE, C. SCHOLZ and R. TURNER (1977): Prediction of the Haycheng earthquake, *EOS, Trans. Am. Geophys. Union*, **58** (5), 236-272.
- RICE, J.R. and J.W. RUDNICKI (1979): Earthquake precursor effects due to pore fluid stabilization of a weakening fault zone, *J. Geophys. Res.*, **84** (B5), 2177-2193.
- RIKITAKE, T. (1976): *Earthquake Prediction* (Elsevier Scientific Publishing Company, Amsterdam-Oxford-New-York), pp. 388.
- RIKITAKE, T. (1988): Earthquake prediction: an empirical approach, *Tectonophysics*, **148** (3-4), 195-210.
- RIKITAKE, T. and Y. YAMAZAKI (1985): The nature of resistivity precursor, *J. Earthquake Pred. Res.*, **3**, 559-570.
- ROELOFFS, E.A. (1988): Hydrologic precursors to earthquakes: a review, *Pure Appl. Geophys.*, **126** (2-4), 177-209.
- SADOVSKII, M.A., L.G. BOLKHOVITINOV and V.F. PISARENKO, (1987): *Deformatsiya Zemnoi Kory i Seismicheskii Protseess* (Nauka, Moscow), pp. 100.
- SPICHAK, V.V., E.B. FAINBERG and Y.P. SIZOV (Editors) (2002): *III International Workshop on Magnetic, Electric and ElectroMagnetic Methods in Seismology and Volcanology (MEEMSV-2002), Scientific Program and Abstracts*, Moscow, pp. 257.
- SYKES, L.R., B.E. SHAW and C.H. SCHOLZ (1999): Rethinking earthquake prediction, *Pure Appl. Geophys.*, **155**, 207-232.
- TENG, T., L. SUN and J.K. MCRANEY (1981): Correlation of groundwater radon anomalies with earthquakes in the Greater Palmdale Bulge area, *Geophys. Res. Lett.*, **8** (5), 441-444.
- TOMASCHEK, R. (1955): Earth tilts in the British islands connected with far distant earthquakes, *Nature*, **176** (4470), 24-25.
- TRAMUTOLI, V., G. DI BELLO, N. PERGOLA and S. PISCITELLI (2001): Robust satellite techniques for remote sensing of seismicallly active areas, *Ann. Geofis.*, **44** (2), 295-312.
- TSUBOI, C. (1956): Earthquake energy, earthquake volume, aftershock area, and strength of the earth's crust, *J. Phys. Earthquake*, **4** (2), 63-66.
- ULOMOV, V.I. (1987): On the relation of the sizes of focus and preparation zone of earthquakes, *Dokl. Usbek Acad. Sci.*, **9**, 39-40.
- UYEDA, S., T. NAGAO, Y. ORIHARA and I. TAKAHASHI (2000): Geoelectric potential changes; possible precursors to earthquakes in Japan, *Proc. Nat. Acad. Sci.*, **97**, 4561-4566.
- VAROTSOS, P., K. ALEXOPOULOS and M. LAZARIDOU (1993): Latest aspects of EQ prediction in Greece based on seismic electric signals, *Tectonophysics*, **224**, 1-38.
- WAKITA, H., Y. NAKAMURA and Y. SANO (1998): Short-term and intermediate-term geochemical precursors, *Pure Appl. Geophys.*, **126** (2-4), 267-278.
- WARWICK, J.W., C. STOKER and T.R. MAYER (1982): Radio emission associated with rock fracture: possible application to great Chilean earthquake of May 22, *J. Geophys. Res.*, **4**, 2851-2859.
- WESSON, R.L. and C. NICHOLSON (1988): Intermediate-term pre-earthquake phenomena in California, 1975-1986, and preliminary forecast of seismicity for the next decade, *Pure Appl. Geophys.*, **126** (2-4), 407-446.
- WIDEMAN, C.J. and M.W. MAJOR (1967): Strain steps asso-



- ciated with earthquakes, *Bull. Seismol. Soc. Am.*, **57** (6), 1429-1444.
- WYATT, F.K., D.C. AGNEW and M. GLADVIN (1994): Continuous measurements of crustal deformation for the 1992 landers earthquake sequence, *Bull. Seismol. Soc. Am.*, **84** (3), 768-779.
- YAMADA, J. (1973): A water-tube tiltmeter and its applications to crustal movement studies, *Spec. Bull. Earthquake Res. Inst., Univ. Tokyo*, **10**, part 1.
- YAMAZAKI, Y. (1977): Tectonoelectricity, *Geophys. Surv.*, **3**, 123-142.
- YAMAZAKI, Y. (1983): Pre-seismic resistivity changes recorded by the resistivity variometer, *Bull. Earthquake Res. Inst., Univ. Tokyo*, **58**, part 2, 477-525.
- YOSHINO, T., I. TOMIZAWA and T. SIGIMOTO (1992): Results of statistical analysis of LF seismogenic emissions as precursors to the earthquake and volcanic eruptions, *Res. Lett. Atmos. Electr.*, **12**, 203-210.
- YOSHINO, T., H. UTADA and T. YUKUTAKE (1998): Variations in Earth resistivity at Aburatsubo, Central Japan (1983-1997), *Bull. Earthquake Res. Inst., Univ. Tokyo*, **73**, part 1, 1-72.